JOURNAL OF MATERIALS SCIENCE 30 (1995) 1642–1652

Compressive strength of a rigid-rod polymer fibre embedded in an isotropic matrix

R. HENTSCHKE, M. J. KOTELYANSKII
Max-Planck-Institut für Polymerforschung, Ackermannweg 10, 55128 Mainz, Germany

The results are presented of an approximate elastic stability analysis for an anisotropic polymer fibre under compressive stress, which is embedded in an isotropic elastic matrix. This case, which thus far has not been treated properly, corresponds most closely to the experiments, which yield the best quantitative measurements of the compressive strength of high-modulus polymer fibres. Within the limits of a weak matrix, i.e. the shear modulus of the matrix is small compared to the shear modulus of the fibre, a simple analytical formula has been obtained for the compressive strength of the fibre in terms of its longitudinal Young's modulus, and the Poisson's ratio and shear modulus of the matrix. On the other hand, for a strong matrix the compressive strength of the fibre is solely determined by its shear modulus. For the intermediate regime, a simple but highly accurate interpolating expression has been constructed.

1. Introduction

Aramid fibres based on poly(*p*-phenylene terephthalamide) (PPTA), polybenzamide (PBA) and other high-strength, high-modulus, rigid-rod polymer fibres, have impressive tensile strength at low specific weight [1]. The good tensile properties result from a high degree of molecular alignment, which is favoured by the rigid-rod character of the molecules. The compressive strength of these materials, however, is typically less than 25% of their corresponding tensile strength. Thus, there is a significant interest in increasing the compressive strength of rigid-rod polymer fibres without, at the same time, diminishing their tensile strength (see, for instance [1–3]). Quite a number of experimental, theoretical and combined studies, with the theoretical approaches both on the molecular level [4–6] and in terms of continuum approaches [4, 7] based on elastic stability arguments [8, 9], have focused on this problem [7, 10–16]. Despite this, however, compressive failure in rigid-rod polymer fibres is still not very well understood.

Experimentally, the onset of compressive failure manifests itself in the formation of kink bands (localized deformation concentrations) along the fibre. Interestingly, most electron micrographs of fibres exhibiting kink bands, suggest a quasi-periodic inter kink band distance [4, 7, 10] rather than a completely irregular spacing as one might expect if the kink band formation was tied to random defects. Thus it is not unreasonable to expect compressive failure to be initiated at a certain wavelength, which can be derived from elastic buckling theories [8, 9]. The simplest of these is the Euler buckling of slender isolated rods [8, 9] which predicts a critical compressive strength, σ_c, proportional to $\lambda_{zzzz} q_c^2$, where λ_{zzzz} is the longitudinal Young's modulus, $q_c \sim 1/L$ is the critical buckling wave vector, and L is the rod length. Even though a sinusoidal buckling pattern may be observed in polymer fibre composites [17], this simple model is not really applicable to these cases. For instance, the buckling is typically not observed with the smallest q as this model predicts. Also, it is not clear what L really is. If L simply is taken to be the fibre length, then σ_c usually is hopelessly small. The same is obviously true if the Euler formula is applied on the molecular level and L is taken to be the chain length. On the other hand, one can get within a factor of two to three of the experimental σ_c by identifying L with the wavelength of the surface ripple structures in skin-peeling experiments on Kevlar 49 and PBO fibres [15]. But it is difficult to justify this definition of L. Most of these problems arise because the simple Euler buckling model applies to isolated fibres, whereas typically a fibre is embedded in an anisotropic network of other fibres or in a more or less isotropic composite matrix. A simple theoretical model, which is supposed to take this into account, is the "beam on an elastic foundation" [8, 9]. This model, which simply includes the elastic response of the matrix by a term proportional to the square of the lateral fibre displacement, yields a critical compressive strength of the form $\sigma_c = \sigma_E + Cq_c^{-2}$, where σ_E is the above Euler contribution and C describes the stiffness of the foundation (or matrix). Thus, here the critical q_c is finite and proportional to $(C/\lambda_{zzzz})^{1/4}$. Therefore, the critical strength can assume any value governed by the size of C, and the corresponding wavelength might be compared with the experimental inter kink band distance at the onset of compressive failure. Notice also that in this model L does not appear in the final expression for σ_c, explicitly. However, the authors are only aware of calculations, where C is an *ad hoc*

0022–2461

constant rather than being calculated in terms of the elastic constants of the matrix material (even though C sometimes is identified with the transverse modulus of the foundation [9]). Another shortcoming of this extended model is that it cannot account for the simple relation $\sigma_c \approx G/3$, where G is the longitudinal shear modulus of the fibre, which seems to be obeyed by a number of different anisotropic fibres [12, 18]. The shear independence of above buckling models holds only under conditions when $\sigma_E \ll G$. Two simple extensions of the Euler theory for isolated beams taking shear corrections into account (for vanishing Poisson's ratio) are

$$\sigma_c = \left[\left(1 + \frac{4n\sigma_E}{G}\right)^{1/2} - 1\right]\frac{G}{2n} \tag{1}$$

and

$$\sigma_c = \frac{\sigma_E}{1 + n\sigma_E/G} \tag{2}$$

where n is a constant, which depends on the beam cross-section ($n \approx 1.1$ for circular cross-sections and $n \approx 1.2$ for rectangular cross-sections) [9]. Note that for $\sigma_E \ll G$, both expressions show the same limiting behaviour, i.e. $\sigma_c \sim \sigma_E(1 - n\sigma_E/G)$, which for solid slender isotropic columns is the relevant limit. Thus shear reduces the compressive strength. If we consider the opposite limit, i.e. $\sigma_E \gg G$, by-passing momentarily the question of the validity of the above expressions in this limit, we obtain the leading behaviour $\sigma_c \sim (\sigma_E G/n)^{1/2}$ and $\sigma_c \sim G/n$, respectively. Notice that the second expression would indicate a behaviour similar to what is observed, even though n is too small. Notice also that if we can combine the second shear correction expression, i.e. Equation 2, with the elastic foundation model, which prevents the critical q from becoming small for large L, then the limit $\sigma_E \gg G$ is not at all unrealistic for rigid-rod polymers for which $\lambda_{zzzz} \gg G$. However, Zwaag *et al.* [7] show the *ad hoc* combination of the second shear correction expression with σ_E calculated according to the above "beam on an elastic foundation" model, to overestimate by about a factor of three, the compressive strength of an aramide fibre embedded in epoxy. Nevertheless, the basic form of the second shear correction expression is appealing, because it combines the two limiting cases into one expression. Thus, it is worth exploring whether this or a similar expression for σ_c can be derived somewhat more formally including the embedding matrix in terms of its elastic constants. It is also worth adding that the fibre failure can be thought of in terms of cooperative modes on the chain level. Extending an analysis of Rosen [19], DeTeresa *et al.* [4] have investigated two different cooperative failure modes one giving the same result as the foundation model and the other giving $\sigma_c = G$.

In this work, an elastic stability analysis was carried out of a rigid-rod polymer fibre based on the standard expression for the elastic free energy of the uniaxial anisotropic solid. The two main assumptions, which were used to simplify the problem, are two-dimensionality, i.e. only the plane of bending, and $u(x, z) = u(z)$, where $u(z)$ is the fibre displacement along z, the direction perpendicular to direction of the unbuckled fibre axis, x, are considered. The two-dimensional fibre is embedded in an isotropic matrix characterized by its shear modulus, μ, and Poisson's ratio, ν. In the two limits for weak and strong matrices analytical expressions for σ_c are obtained from which we construct a simple interpolating expression, given by

$$\sigma_c = \frac{\sigma_E}{1 + \sigma_E/G} + \frac{2\mu}{(1 - \nu)q_c b} \tag{3}$$

where q_c corresponds to the minimum of $\sigma(q)$, and b is the fibre width. By comparing this expression to the numerical solutions, we show that the interpolation approximation is indeed a very good one. In addition, we study the crossover between the region where σ_c is a strong function of the matrix elasticity and the region where $\sigma_c \approx G$. Finally, we discuss the theoretical predictions in the context of the available experimental data.

2. Elastic instability of the isolated anisotropic fibre

Consider an isolated uniaxially anisotropic fibre, which becomes unstable due to an external axial compressive stress. The total potential energy of the fibre is given by

$$\pi_{\text{fibre}} = \int_0^L \int_{-b/2}^{b/2} H \, dx dz \tag{4}$$

where L is the length and b is the width of the fibre in the plane of bending (cf. Fig. 1), i.e. the plane of bending is the xz-plane and the y-direction is omitted. The integrand is

$$\begin{aligned} H = & -\frac{\sigma}{2}\left[\frac{\partial}{\partial z}u(x,z)\right]^2 + \frac{1}{2}\lambda_{zzzz}\left[\frac{\partial}{\partial z}w(x,z)\right]^2 \\ & \times (2\lambda_{\xi\eta\xi\eta} + \lambda_{\xi\xi\eta\eta})\left[\frac{\partial}{\partial x}u(x,z)\right]^2 \\ & + 2\lambda_{\xi\eta zz}\frac{\partial}{\partial z}w(x.z)\frac{\partial}{\partial x}u(x,z) \\ & + \lambda_{\xi z\eta z}\left[\frac{\partial}{\partial z}u(x.z)\frac{\partial}{\partial x}w(x,z)\right]^2 \end{aligned} \tag{5}$$

where the first term is the work done by the compressive stress, σ, along z and the remainder is the elastic

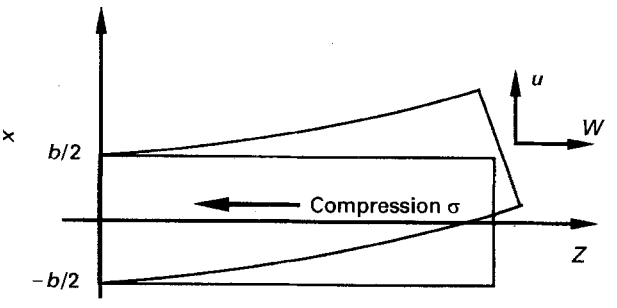

Figure 1 Schematic illustration of a section of the unbent and the bent fibre characterized by the displacements u along x and w along z.

free energy for the case of a material with uniaxial symmetry [8]. The five λs are the elastic constants of the uniaxially anisotropic material.

The second main assumption is

$$u(x, z) = u(z) \tag{6}$$

which is known to be quite reasonable for slender beams [8]. Notice that due to the two-dimensional formulation of the model and the assumed x-independence of $u(z)$, there are only two remaining elastic constants, i.e.

$$H = -\frac{1}{2}\sigma\left[\frac{\partial}{\partial z}u(z)\right]^2 + \frac{1}{2}\lambda_{zzzz}\left[\frac{\partial}{\partial z}w(x, z)\right]^2 + \lambda_{\xi z\eta z}\left[\frac{\partial}{\partial x}w(x, z) + \frac{\partial}{\partial z}u(z)\right]^2 \tag{7}$$

Notice also that H can be mapped on to the corresponding isotropic case via $\lambda_{zzzz}/2 = \lambda/2 + \mu$ and $\lambda_{\xi z\eta z} = \mu/2$, where λ is the Lamé coefficient and μ is the isotropic shear modulus. By writing the displacement field $w(x, z)$ as

$$w(x, z) = -x\frac{\partial}{\partial z}u(z) + w_1(x, z) \tag{8}$$

where $w_1(x, z) = 0$ leads to the simple shearless Euler buckling of slender columns (see below), H thus becomes

$$H = -\frac{1}{2}\sigma\left[\frac{\partial}{\partial z}u(z)\right]^2 + \frac{1}{2}\lambda_{zzzz}\left[-x\frac{\partial^2}{\partial z^2}u(z) + \frac{\partial}{\partial z}w_1(x, z)\right]^2 + \lambda_{\xi z\eta z}\left[\frac{\partial}{\partial x}w_1(x, z)\right]^2 \tag{9}$$

The goal is to minimize the fibre potential energy for this approximation of H, where the minimization has to comply with the conditions

$$\sigma_{ik}n_k = 0 \tag{10}$$

where

$$\sigma_{ik} = \frac{\partial H}{\partial u_{ik}} \tag{11}$$

for the surface stress components, σ_{ij}, along the free surface of the fibre. Here n_k is the kth component of the surface normal vector. Because the y-direction is excluded and because clamped fibre ends is assumed, the only remaining equations are those where $k = x$. Notice, however, that σ_{xx} does not appear here, because the approximate H does not depend on $u_{xx} = \partial u/\partial x$. Thus the only boundary condition is

$$\sigma_{xz}\Big|_{x=\frac{\pm b}{2}} = 0 \tag{12}$$

i.e.

$$8\lambda_{\xi z\eta z}\frac{1}{2}\left[\frac{\partial}{\partial z}u(z) + \frac{\partial}{\partial x}w(x, z)\right]\Bigg|_{x=\frac{\pm b}{2}} = 4\lambda_{\xi z\eta z}\frac{\partial}{\partial x}w_1(x, z)\Big|_{x=\frac{\pm b}{2}} = 0 \tag{13}$$

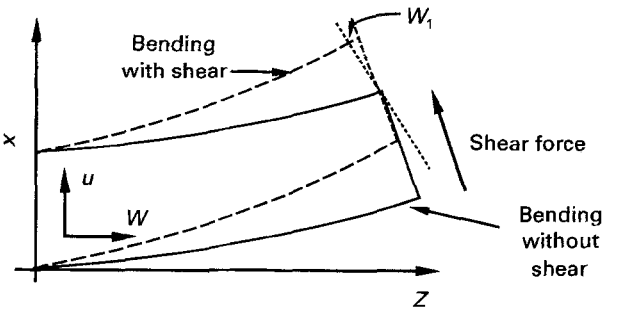

Figure 2 Schematic illustration of the effect of shear on the fibre cross-section.

2.1. The fibre profile

In order to proceed, a reasonable approximation must be made for $w_1(x, z)$. Notice that the shear force acts parallel to the cross-sectional plane and thus predominantly increases the deflection $\partial u(z)/\partial z$ without, at the same time, increasing the displacement along x (see Fig. 2). Thus, to a first approximation, the effect of the shear correction is to yield a reduced effective deflection, i.e.

$$w(x, z) = -x\left[\frac{\partial}{\partial z}u(z) - \varepsilon(x)\frac{\partial}{\partial z}u(z)\right] \tag{14}$$

so that

$$w_1(x, z) = x\varepsilon(x)\frac{\partial}{\partial z}u(z) \tag{15}$$

With this we obtain for the fibre potential energy

$$\pi_{\text{fibre}} = \int_0^L\int_{-b/2}^{b/2} -\frac{1}{2}\sigma\left[\frac{\partial}{\partial z}u(z)\right]^2 + \frac{1}{2}\lambda_{zzzz}\left[\frac{\partial^2}{\partial z^2}u(z)\right]^2 x^2[1 - \varepsilon(x)]^2 + \lambda_{\xi z\eta z}\left[x\frac{\partial}{\partial x}\varepsilon(x) + \varepsilon(x)\right]^2\left[\frac{\partial}{\partial z}u(z)\right]^2 dz\,dx \tag{16}$$

and the above boundary condition becomes

$$4\lambda_{\xi z\eta z}\frac{\partial}{\partial z}u(z)\left[x\frac{\partial}{\partial x}\varepsilon(x) + \varepsilon(x)\right]\Bigg|_{x=\frac{\pm b}{2}} = 0 \tag{17}$$

Note that by symmetry, i.e. both sides of the fibre are identical, $\varepsilon(x)$ should be an even function of x. Here $\varepsilon(x)$ is written as a polynomial in even powers of x/b, i.e.

$$\varepsilon(x) = \varepsilon_0 + \varepsilon_2\left(\frac{x}{b}\right)^2 + \ldots = \sum_{k=0}^{n}\varepsilon_{2k}\left(\frac{x}{b}\right)^{2k} \tag{18}$$

2.2. Single-mode buckling

Assuming that the elastic failure of the fibre can be described in terms of a single wave vector $q = 2\pi j/L$ ($j = 1, \ldots$) gives

$$u(z) = u_0[1 - \cos(qz)] \tag{19}$$

Note that for $j = 0$ there is no displacement. With this we obtain

$$\pi_{\text{fibre}} = \frac{Lbq^2u_0^2}{4}\left(-\sigma + \frac{\lambda_{zzzz}b^2q^2}{12}\right) - \sum_{k=0}^{n}\frac{L\lambda_{zzzz}b^3q^4}{4^{k+2}(2k+3)}(u_0^2\varepsilon_{2k}) - \sum_{k'=0}^{n}\frac{L\lambda_{zzzz}b^3q^4}{4^{k'+2}(2k'+3)}(u_0^2\varepsilon_{2k'}) + \sum_{k=0}^{n}\sum_{k'=0}^{n}\varepsilon_{2k}\varepsilon_{2k'}u_0^2\left[\frac{L\lambda_{zzzz}b^3q^4}{4^{k+k'+2}(2k+2k'+3)} + \frac{2Lb\lambda_{\xi\eta z}q^2(4kk'+2k+2k'+1)}{4^{k'+k+1}(2k+2k'+1)}\right] \tag{20}$$

or in matrix form

$$\pi_{\text{fibre}} = \begin{bmatrix} u_0 \\ \varepsilon'_{2k'} \end{bmatrix}^T \begin{Bmatrix} \frac{Lbq^2}{4}\left(-\sigma + \frac{\lambda_{zzzz}b^2q^2}{12}\right) & -\frac{L\lambda_{zzzz}b^3q^4}{4^{k'+2}(2k'+3)} \\ -\frac{L\lambda_{zzzz}b^3q^4}{4^{k+2}(2k+3)} & \left[\frac{L\lambda_{zzzz}b^3q^4}{4^{k+k'+2}(2k+2k'+3)} + \frac{2Lb\lambda_{\xi\eta z}q^2(4kk'+2k+2k'+1)}{4^{k'+k+1}(2k+2k'+1)}\right] \end{Bmatrix} \begin{bmatrix} u_0 \\ \varepsilon_{2k} \end{bmatrix} \tag{21}$$

where $\varepsilon'_{2k} = \varepsilon_{2k}u_0$ denotes a sequence of coefficients with $k = 0, 1, \ldots, n$.

The amplitude vector can be found as well as the critical compressive strength, σ_c, from the condition

$$\delta(\pi_{\text{fibre}} + \tau g) = 0 \tag{22}$$

where τ is a Lagrange parameter conjugate to the boundary condition

$$g = \sum_{k=0}^{n}\frac{q\lambda_{\xi\eta z}(2k+1)}{2^{2k-2}}\varepsilon'_{2k} = 0 \tag{23}$$

Again, writing Equation 22 in matrix notation,

$$\pi = \mathbf{v}^+ M\mathbf{v} \tag{24}$$

where $\mathbf{v} = [u_0\, \varepsilon'_0\, \varepsilon'_2 .. \varepsilon'_{2n}\, \tau]$ and

$$M = \begin{bmatrix} \pi_{\text{fibre11}} & \pi_{\text{fibre12}} & 0 \\ \pi_{\text{fibre21}} & \pi_{\text{fibre22}} & \frac{q\lambda_{\xi\eta z}(2k+1)}{2^{2k-2}} \\ 0 & \frac{q\lambda_{\xi\eta z}(2k'+1)}{2^{2k'-2}} & 0 \end{bmatrix} \tag{25}$$

Notice that M is a real symmetric $(2+n)\times(2+n)$ matrix. The onset of compressive failure is then equivalent to the condition

$$\det(M) = 0 \tag{26}$$

This is because we can write

$$\pi = \mathbf{v}^+ M\mathbf{v} = \mathbf{v}^+ SS^+ MSS^+\mathbf{v} = \sum_j \lambda_j(\mathbf{v}^+ S)_j^2 \tag{27}$$

where $SS^+ = \mathbf{1}$, and $\mathbf{1}$ is the identity matrix. Here the λ_j are the eigenvalues of M (not to be confused with the elastic constants). Clearly, the amplitude of π diverges if one λ_j turns negative – which means that the fibre fails.

3. The isolated fibre compared to the fibre on an elastic foundation

Before Equation 26 is discussed, one additional aspect must be included. The above approach always yields the smallest possible critical q given by $2\pi/L$ – as will be seen. However, this is not necessarily the correct one for a fibre, which is not isolated but has lateral support. A common extension is the case of a beam (fibre) on an elastic foundation, where the foundation is included in the above elastic free energy (cf. Equation 7) via a term proportional to u^2, i.e.

$$H = -\frac{1}{2}\sigma\left[\frac{\partial}{\partial z}u(z)\right]^2 + \frac{1}{2}\lambda_{zzzz}\left[\frac{\partial}{\partial z}w(x,z)\right]^2 + \lambda_{\xi\eta z}\left[\frac{\partial}{\partial x}w(x,z) + \frac{\partial}{\partial z}u(z)\right]^2 + \frac{1}{2}C\left(\frac{u(z)}{b}\right)^2 \tag{28}$$

where C describes the elastic stiffness of the lateral support. A calculation analogous to that for the isolated fibre shows that the only difference is that now

$$\pi_{\text{fibre11}} = \frac{Lbq^2}{4}\left[-\sigma + \frac{\lambda_{zzzz}b^2q^2}{12} + 3\frac{C}{b^2q^2}\right] \tag{29}$$

Using Equation 29 instead of the 11-entry in Equation 21, we finally obtain the critical σ by solving Equation 26 for $\sigma(q)$, where

$$\sigma_c = \sigma(q_c) \tag{30}$$

and q_c follows from

$$\left.\frac{\partial\sigma}{\partial q}\right|_{q=q_c} = 0 \tag{31}$$

Here the computer program Mathematica [20] is used to solve analytically Equation 26 for $\sigma(q)$ as well as for all other calculations.

For the simplest case, $n = 0$, the classical textbook result is obtained

$$\sigma = \sigma_E + 3\frac{C}{b^2q^2} \tag{32}$$

where

$$\sigma_E = \frac{\lambda_{zzzz} b^2 q^2}{12} \tag{33}$$

and

$$bq_c = \left[36 \frac{C}{\lambda_{zzzz}}\right]^{1/4} \tag{34}$$

Notice that σ_E is commonly written in terms of the moment of inertia of the fibre cross-section, given for example, by $b^4/12$ for a square fibre cross-section.

The next slightly more complicated case is $n = 1$, which yields

$$\sigma = \sigma_E \Big/ \left(1 + \frac{17}{14}\frac{\sigma_E}{G}\right)\left(1 + \frac{1}{70}\frac{\sigma_E}{G}\right) + \frac{3C}{b^2q^2} \tag{35}$$

where $G = 2\lambda_{\xi z \eta z}$. Here shear corrections begin to appear. Notice that for $C = 0$ an expression is obtained which is very close to another textbook result, i.e. Equation 2, discussed in Section 1. In fact, the expansion of Equation 35 to second order in σ_E yields $\sigma = \sigma_E$ (1–1.2 σ_E/G), which is identical to the corresponding expansion of Equation 2 for the case of rectangular cross-sections. Thus, taking shear into account leads to a reduced compressive strength.

Instead of trying to work out the critical q for this formula, it is more useful to look at what happens for even higher n. Because the expressions for σ become increasingly complicated we turn to a discussion in terms of numerical examples. Figs 3 and 4 show σ/G as obtained from Equation 26 as a function of qb for $n = 0, 1, 3, 5, 7$. Note that the stiffness $C = 0$ in Fig. 3, whereas in Fig. 4 we have $C > 0$. For $C = 0$ the critical q is always $2\pi/L$, as anticipated. For $C > 0$ the critical q is no longer necessarily $2\pi/L$. Notice also that what used to be the second shear correction for $C = 0$ (i.e. Equation 2), is now the same expression but with σ_E replaced by $\sigma_E + 3C/(bq)^2$ as elsewhere [7]. Clearly, the effect of increasing C is that both the critical compressive strength, i.e. minimum of σ, as well as the corresponding critical q, are increased. But the presence of shear always ensures that σ_c is bounded from

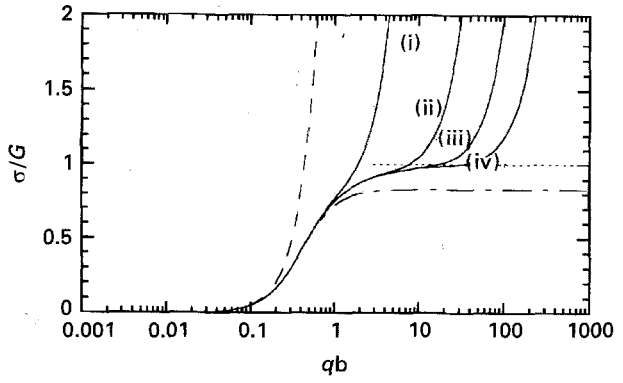

Figure 3 Fibre compressive strength, σ, divided by the fibre shear modulus G versus the reduced wave vector qb for the isolated fibre. The different lines are for $n = (- - -)0$, (i) 1, (ii) 3, (iii) 5, (iv) 7 compared to the second shear correction Equation 2 discussed in Section 1 (— — —). The curve for $n = 0$ is identical to the simple Euler buckling of a rod with clamped ends. Notice that here $\lambda_{zzzz} = 123$ GPa and $\lambda_{\xi z \eta z} = 1$ GPa, which roughly corresponds to Kevlar [18].

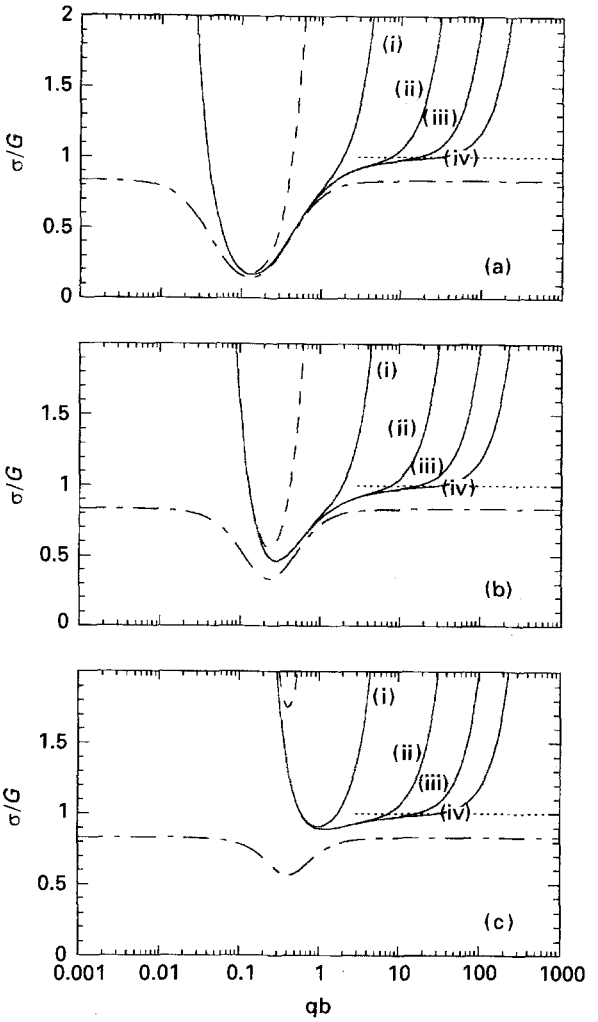

Figure 4 σ/G versus qb for $n = (- - -)0$, (i) 1, (ii) 3, (iii) 5, (iv) 7 as in Fig. 3 but for $C \neq 0$, i.e. $C =$ (a) 0.001 GPa, (b) 0.01 GPa, (c) 0.1 GPa. (- - -) The second shear correction Equation 2 discussed in Section 1 but with σ_E replaced by $\sigma_E + 3C/(bq)^2$ as in [7]. As in Fig. 3, $\lambda_{zzzz} = 123$ GPa and $\lambda_{\xi z \eta z} = 1$ GPa.

above by the shear modulus. The problem with this approach is that adding the C-term is an *ad hoc* addition, and, in particular, it is unclear how C relates to the elastic constants of the medium in which the fibre is embedded.

4. The displacement field and the elastic potential energy in an embedding infinite isotropic medium

Here the embedded fibre is treated more formally. The goal is to derive an expression for

$$\pi_{total} = \pi_{fibre} + \pi_{matrix} \tag{36}$$

We already have an expression for the fibre contribution to the total potential energy, and thus here an expression is derived for the matrix contribution. In addition, the fibre–matrix interface is then dealt with assuming a tight cohesion between the fibre and the matrix, i.e. the displacements in the two media are identical at the interface. In order to calculate π_{matrix} the fibre-induced displacement field inside the matrix must be known, which obeys the equilibrium

condition (cf. [8])

$$\nabla^2\boldsymbol{\omega} + \frac{1}{1-2\nu}\nabla\nabla\,\omega = 0 \tag{37}$$

where $\boldsymbol{\omega} = (u, w)$ and $\nabla\nabla\cdot\boldsymbol{\omega}$ = grad div $\boldsymbol{\omega}$, or in terms of the components

$$(1+\Omega)\frac{\partial^2}{\partial x^2}u(x,z) + \frac{\partial^2}{\partial z^2}u(x,z) + \Omega\frac{\partial^2}{\partial x\partial z}w(x,z) = 0 \tag{38}$$

and

$$(1+\Omega)\frac{\partial^2}{\partial z^2}w(x,z) + \frac{\partial^2}{\partial x^2}w(x,z) + \Omega\frac{\partial^2}{\partial z\partial x}u(x,z) = 0 \tag{39}$$

where $\Omega = 1/(1-2\nu)$ and ν is the Poisson's ratio of the matrix material. The somewhat lengthy but straightforward solution of this set of equations is contained in the Appendix. Here we merely state the final result for the matrix potential energy, i.e.

$$\pi_{\text{matrix}} = \begin{bmatrix} c_1 \\ c_2 \end{bmatrix}\begin{bmatrix} \pi_{\text{matrix11}} & \pi_{\text{matrix12}} \\ \pi_{\text{matrix12}} & \pi_{\text{matrix22}} \end{bmatrix}\begin{bmatrix} c_1 \\ c_2 \end{bmatrix} \tag{40}$$

where

$$\pi_{\text{matrix11}} = \frac{4Lq}{\Omega^2 e^{bq}} \times\left\{\lambda + \mu\left[2\Omega(\Omega+2) + \Omega(3\Omega+2)(bq+1) + \frac{\Omega^2 b^2 q^2}{2} + 3\right]\right\} \tag{41}$$

$$\pi_{\text{matrix22}} = \frac{4L}{q\Omega^2 e^{bq}}\left\{\lambda + \mu\left[\Omega(\Omega+2)(bq+1) + \frac{\Omega^2 b^2 q^2}{2} + 3\right]\right\} \tag{42}$$

$$\pi_{\text{matrix12}} = \frac{4L}{\Omega^2 e^{bq}}\left(\lambda + \mu\left[2\Omega[\Omega+1)(bq+1)+1] + \frac{\Omega^2 b^2 q^2}{2} + 3\right]\right) \tag{43}$$

Notice that $\lambda = 2\Omega\nu\mu$, i.e. λ is the matrix's Lamè coefficient and μ is the matrix's shear modulus. In addition, we have the two equations (cf. Appendix)

$$g + 4\mu q e^{-bq/2}\left(\frac{bq}{2} + \frac{1}{\Omega} + 1\right)c_1 + 2\mu e^{-bq/2}\left(bq + \frac{2}{\Omega}\right)c_2 = 0 \tag{44}$$

and

$$u_0 + 2e^{-bq/2}\left(\frac{bq}{2} + \frac{2}{\Omega} + 2\right)c_1 + \frac{2}{q}e^{-bq/2}\left(\frac{bq}{2} + \frac{2}{\Omega} + 1\right)c_2 = 0 \tag{45}$$

which result from the stress-boundary condition and the equality of the displacements at the fibre–matrix interface, respectively.

5. Elastic instability of the embedded anisotropic fibre

Now everything can be put together and the stress necessary to induce an elastic instability of the embedded fibre with a specific q, can be calculated. The reasoning in this case is completely analogous to the case of the isolated fibre. In addition, there are two constraining equations (44 and 45), which are again included via the method of Lagrange multipliers. As before, we find the compressive strength from Equation 26, where now

$$M = \begin{bmatrix} \pi_{\text{fibre11}} & \pi_{\text{fibre12}} & 0 \\ \pi_{\text{fibre21}} & \pi_{\text{fibre22}} & \frac{q\lambda_{\xi z\eta z}(2k+1)}{2^{2k-2}} \\ 0 & \frac{q\lambda_{\xi z\eta z}(2k+1)}{2^{2k-2}} & 0 \\ 1 & 0 & 0 \\ 0 & 0 & 4\mu q e^{-bq/2}\left(\frac{bq}{2}+\frac{1}{\Omega}+1\right) \\ 0 & 0 & 2\mu e^{-bq/2}\left(bq+\frac{2}{\Omega}\right) \end{bmatrix}$$

$$\begin{bmatrix} 1 & 0 & 0 \\ 0 & 0 & 0 \\ 0 & 4\mu q e^{-bq/2}\left(\frac{bq}{2}+\frac{1}{\Omega}+1\right) & 2\mu e^{-bq/2}\left(bq+\frac{2}{\Omega}\right) \\ 0 & 2e^{-bq/2}\left(\frac{bq}{2}+\frac{2}{\Omega}+2\right) & \frac{2}{q}e^{-bq/2}\left(\frac{bq}{2}+\frac{2}{\Omega}+1\right) \\ 2e^{-bq/2}\left(\frac{bq}{2}+\frac{2}{\Omega}+2\right) & \pi_{\text{matrix11}} & \pi_{\text{matrix12}} \\ \frac{2}{q}e^{-bq/2}\left(\frac{bq}{2}+\frac{2}{\Omega}+1\right) & \pi_{\text{matrix12}} & \pi_{\text{matrix22}} \end{bmatrix} \tag{46}$$

and $\mathbf{v} = [u_0 \varepsilon'_{2k} \tau_1 \tau_2 c_1 c_2]$, where again ε'_{2k} denotes a sequence of coefficients for $k = 0, 1, \ldots, n$, i.e. $\mathbf{v}$ is a $5 + n$-component vector and M is a $(5 + n) \times (5 + n)$ real symmetric matrix. Note also that now τ_1 and τ_2 are both Lagrange parameters conjugate to Equations 44 and 45.

Again, as in the case of the elastic foundation, we must first study a numerical example. As in Figs 3 and 4, we use $\lambda_{zzzz} = 123\,\text{GPa}$ and $\lambda_{\xi z \eta z} = 1\,\text{GPa}$. As Fig. 5 shows, the qualitative behaviour of the embedded fibre is very similar to what was obtained above for the *ad hoc* treatment of the fibre on a foundation.

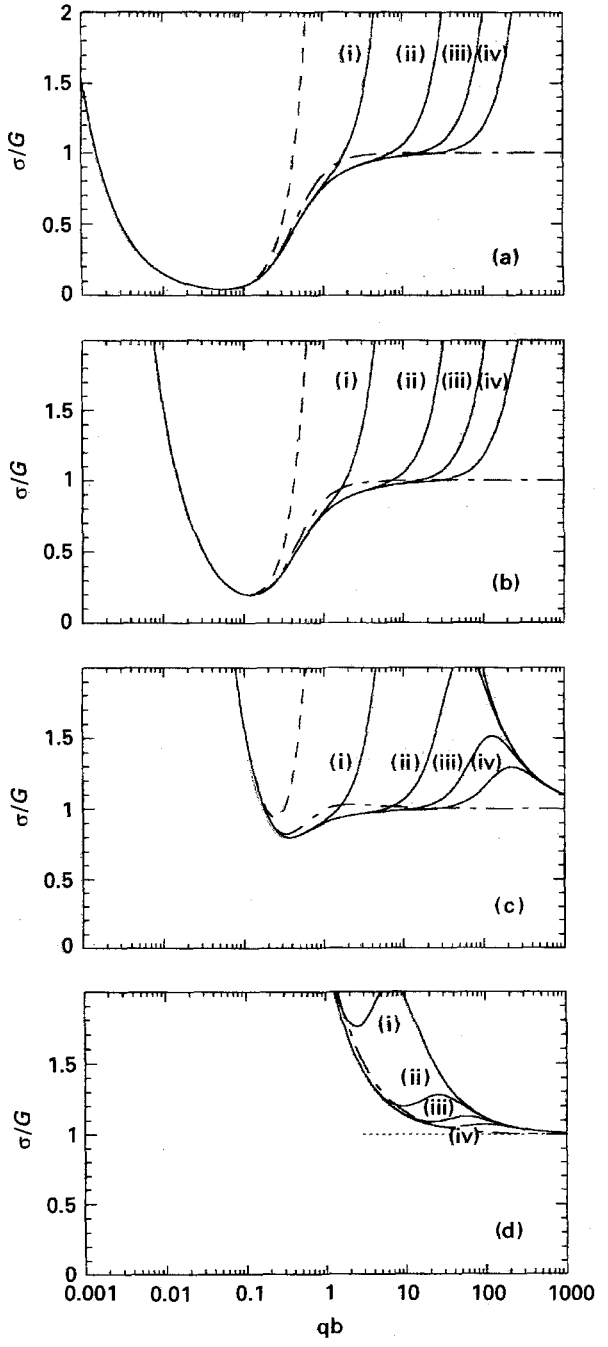

Figure 5 σ/G versus qb for the anisotropic fibre embedded in an isotropic elastic medium for n = (i) 1, (ii) 3, (iii) 5, (iv) 7 and different matrix shear moduli μ, i.e. μ = (a) 0.001 GPa, (b) 0.01 GPa, (c) 0.1 GPa and (d) 1.0 GPa. (– – –) Approximate σ given by Equation 47, (— · —) interpolation Equation 51. As in Figs 3 and 4, $\lambda_{zzzz} = 123$ GPa and $\lambda_{\xi z \eta z} = 1$ GPa. In addition, the Poisson's ratio of the matrix is taken to be $\nu = 0.35$.

Increasing the stiffness of the matrix, which here means increasing μ, increases both the critical σ as well as the attendant q_c. Again, σ_c is bounded by the fibre shear modulus G equal to $2\lambda_{\xi z \eta z}$.

We can calculate analytical expressions for the compressive strength of the fibre within the matrix in certain limiting cases. First we take the result for $n = 1$ and expand it in terms of the fibre shear modulus, μ, as well as in terms of σ_E to lowest order. We obtain the simple result

$$\sigma = \sigma_E + \frac{2\mu}{(1-\nu)qb} \tag{47}$$

for which

$$q_c b = \left(\frac{12}{\lambda_{zzzz}} \frac{\mu}{1-\nu}\right)^{1/3} \tag{48}$$

Notice that q_c scales as $\lambda_{zzzz}^{1/3}$ rather than as $\lambda_{zzzz}^{1/4}$ in the case of the foundation. The performance of this approximation is illustrated in Fig. 5. If we take into account higher order corrections we obtain

$$\sigma = \sigma_E + \frac{2\mu}{(1-\nu)qb} - \frac{6}{5}\frac{\sigma_E^2}{G} + \frac{51}{35}\frac{\sigma_E^3}{G^2} + O(\sigma_E^4, \mu^4) \tag{49}$$

where the corrections now depend on G. The limit for small G (or, what turns out to be the same, for large q), can also be worked out, which yields

$$\sigma = G + \frac{2\mu}{(1-\nu)qb}\left[1 + (3 - 4\nu)\frac{G^2}{\mu^2}\right] + O(G^3) \tag{50}$$

The two formulas hold for all n investigated (the maximum n in our case is 7).

Because even for $n = 1$ the expression for σ is somewhat complicated, it is desirable to have a simple approximate expression for the entire q-range. There are several conceivable interpolations between the two limiting cases. One, which is simple and rather accurate (as shown in Fig. 5), is given by

$$\sigma = \frac{\sigma_E}{1 + \sigma_E/G} + \frac{2\mu}{(1-\nu)qb} \tag{51}$$

Notice that here the matrix enters through one effective parameter, $\mu/(1-\nu)$, only. Assuming the continuum limit (i.e. $L \to \infty$), the critical q can be obtained from $\partial\sigma(q)/\partial q = 0$, i.e.

$$\left(q^4 - \frac{2}{AB}q^3 + \frac{2}{A}q^2 + \frac{1}{A^2}\right) \Big/ [q^2(1 + Aq^2)] = 0 \tag{52}$$

where

$$A = \frac{\sigma_E}{Gq^2} \tag{53}$$

and

$$B = \frac{2\mu}{Gb(1-\nu)} \tag{54}$$

For a weak matrix, i.e. μ is small and thus $1/B$ is large, we have $q_c = [B/(2A)]^{1/3}$ in agreement with Equation 48. For a strong matrix, i.e. μ is large and thus $1/B$ is small, the numerator is always positive and q diverges. Thus beyond a certain value for μ one always finds $\sigma_c = G$. Unfortunately, due to the

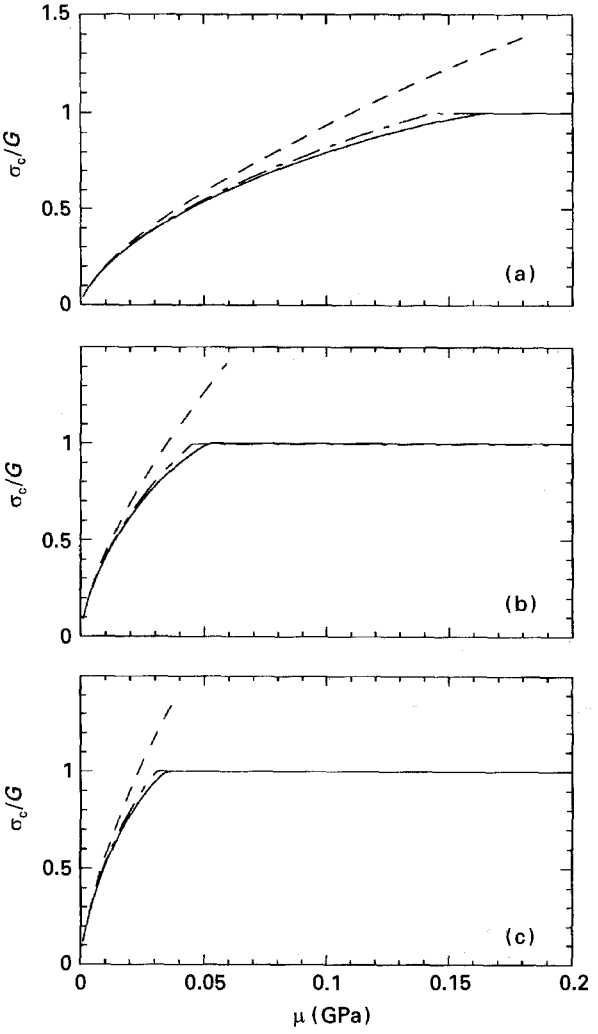

Figure 6 σ_c divided by G versus the matrix shear modulus, μ, for (a) PPTA ($\lambda_{zzzz} = 123$ GPa, $G = 2$ GPa), (b) PBT ($\lambda_{zzzz} = 265$ GPa, $G = 1.2$ GPa), and (c) PE ($\lambda_{zzzz} = 117$ GPa, $G = 0.7$ GPa). (——) $n = 7$, (Equation 51), (– – –) low μ approximation (Equation 47). The values for λ_{zzzz} and G are taken from [18] and [21]. For the matrix's Poisson's ratio we use $\nu = 0.35$.

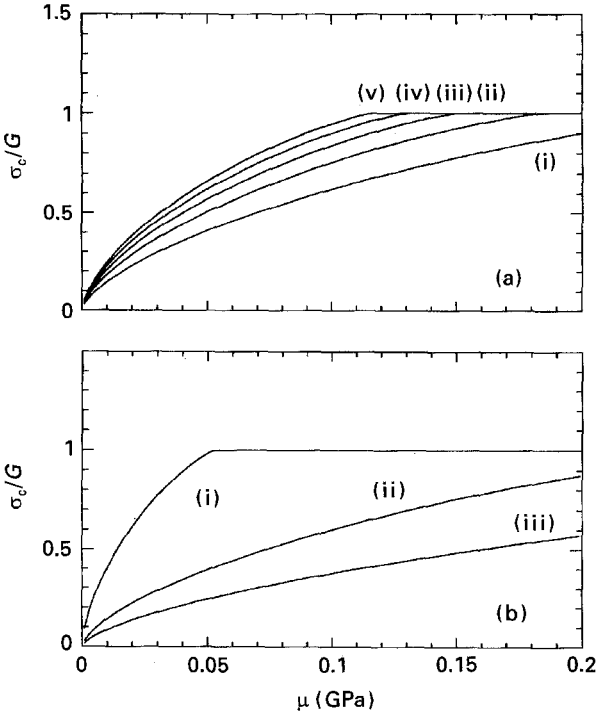

Figure 7 σ_c/G versus the matrix shear modulus, μ. (a) $G = 2$ GPa and λ_{zzzz} = (i) 50 GPa, (ii) 100 GPa, (iii) 150 GPa, (iv) 200 GPa, (v) 250 GPa. (b) $\lambda_{zzzz} = 150$ GPa and G = (i) 1 GPa, (ii) 3GPa, (iii) 5 GPa. The matrix's Poisson's ratio $\nu = 0.35$. All curves are obtained with $n = 7$.

approximate nature of the interpolation, it is not clear whether this "transition" indeed manifests itself in terms of a jump in q_c rather than in a continuous increase. Nevertheless, it is evident that below a certain matrix stiffness, the compressive strength is a strong function of the matrix elastic constants, whereas above a certain matrix stiffness the compressive strength is virtually equal to G, in agreement with previous findings (see below).

However, here Equation 51 allows the crossover to be estimated. Fig. 6 shows the critical fibre compressive strength, σ_c, divided by G as a function of μ for different fibres, i.e. PPTA, poly(*p*-phenyethlene benzobisthiazole) (PBT), and polyethylene (PE). In this plot we compare Equation 51 with the approximation Equation 47 as well as with the solution for $n = 7$. Evidently, the interpolation Equation 51 performs quite well. Fig. 6 also allows estimation of how flexible a matrix material can be before the compressive strength of the fibres is diminished. Notice that the matrix's Poisson's ratio, ν, here is taken to be 0.35. However, notice also that Equation 51, which is a good approximation, depends on the matrix's elastic constants only through the ratio $\mu/(1 - \nu)$. Thus, the effect of varying ν can, to a good approximation, be estimated by scaling μ.

Fig. 7 gives a more systematic overview of the critical fibre compressive strength as a function of the stiffness of the surrounding matrix material. For a constant fibre shear modulus, G, Fig. 7a shows that the crossover is shifted to lower values for the matrix shear modulus, μ, as the longitudinal modulus, λ_{zzzz} increases. In Fig. 7b we keep λ_{zzzz} constant and vary G. Here increasing G also increases the μ at the crossover.

6. Conclusion

The compressive strength of a uniaxially anisotropic polymer fibre embedded in an isotropic matrix has been studied. One result of our elastic stability analysis is a simple expression, which describes the critical compressive stress as function of the elastic constants. Another important point is that this analysis allows estimation of to what extent the elastic stability of the fibre is affected by the surrounding matrix. In particular, we can estimate the threshold stiffness of the matrix material below which the measured critical fibre compressive strength varies as a function of the matrix's elastic constants.

In principle, the present model does allow for compressive strengths in the range of the experimental data, which, as was pointed out above, seem to be well described by $G/3$ [18]. From the micrographs of the buckled fibres [18], or from the data on the kink-band density at compressive failure of the embedded fibres

[7], one can see that failure occurs at $qb \approx 0.01$–0.1. These values correspond to $\sigma \approx 0.1G$–$1.0G$ (Fig. 5), giving a reasonable estimate in comparison to the experimentally observed values. Unfortunately, we lack the information necessary to judge whether the gluing of the fibres to their support beams, as described elsewhere [18], might account for the $G/3$ behaviour. However, as Fig. 6 shows, the matrix (glue) shear modulus would have to be rather low. In addition, what is unknown here but as this analysis shows should be considered, is the fibre must be embedded in a "thick enough" coating on the order of $1/q_c$ (cf. the expressions for the matrix displacement field derived in the Appendix) in order to avoid effects due to the finite matrix thickness. Another disturbing point is that the compressive strength of PE appears to be severely overestimated (about five times) by the $G/3$ curve in [18], which would indicate some basic difference from the other fibres tested.

Even though the present model includes the interaction of the fibre with the matrix more accurately as the foundation model, we are nevertheless forced to simplify the calculation by employing two rather crude approximations. Because we ignore the third dimension we cannot estimate the influence of the shape of the fibre cross-section on the compressive strength. However, two shear correction expressions for the buckling of isolated slender columns, i.e. Equations 1 and 2 were discussed in Section 1 [9]. It was found that the difference between a circular and a rectangular cross-section is about 10%. Only, (in the context of fibres) for more exotic cross-sections, such as those of H-beams, does one obtain more significant deviations. A more severe approximation, on the other hand, might be the x-independence of the displacement u. Avoiding this approximation, however, makes the analytical treatment significantly more difficult. For instance, there are additional elastic constants. This might be the reason why, for instance, the experimental PE result deviates so strongly from the systematic behaviour shown by the other fibres. Here a finite element analysis might perhaps be useful.

In this work we have not discussed the role of the internal fibre structure, such as the degree of molecular orientation, the difference in the molecular organization in the skin as compared to the core region of a fibre, the role of inter-molecular interactions such as hydrogen bonding, and possible inelastic processes, such as intra-fibre delamination, fibre–matrix delamination, etc., which differ from material to material and which may depend on processing. These effects are mostly beyond the present approach, with the possible exception of skin–core effects, which might be included by the introduction of surface regions distinguished from the core region by different values of the elastic constants. But more importantly, if we believe the quasi-universal $G/3$ behaviour observed in [18], this would indicate that all non-universal effects enter primarily through the elastic constants of the material, rather than affecting the compressive strength directly. Therefore, checking whether more than the five out of six tested fibres follow this relation could provide valuable insight.

Appendix

In order to solve the equilibrium conditions (Equation 37) we make the Ansatz

$$u(x,z) = \sum_{j=-\infty}^{\infty} \bar{u}(x,q_j) e^{iq_j z} \tag{A1}$$

and

$$w(x,z) = \sum_{j=-\infty}^{\infty} \bar{w}(x,q_j) e^{iq_j z} \tag{A2}$$

which yields

$$(1+\Omega)\frac{\partial^2}{\partial x^2}\bar{u}(x,q_j) - q_j^2 \bar{u}(x,q_j) + i\Omega q_j \frac{\partial}{\partial x}\bar{w}(x,q_j) = 0 \tag{A3}$$

and

$$-(1+\Omega)\, q_j^2\, \bar{w}(x,q_j) + \frac{\partial^2}{\partial x^2}\bar{w}(x,q_j) + i\Omega q_j \frac{\partial}{\partial x}\bar{u}(x,q_j) = 0 \tag{A4}$$

Making the substitutions

$$y_1(x) = \bar{u}(x,q_j);\ y_2(x) = \frac{\partial}{\partial x}\bar{u}(x,q_j);$$

$$y_3(x) = \bar{w}(x,q_j);\ y_4(x) = \frac{\partial}{\partial x}\bar{w}(x,q_j) \tag{A5}$$

we obtain a system of coupled first-order differential equations, i.e.

$$\frac{\partial}{\partial x}\begin{bmatrix} y_1(x) \\ y_2(x) \\ y_3(x) \\ y_4(x) \end{bmatrix} = \begin{bmatrix} 0 & 1 & 0 & 0 \\ \dfrac{q^2}{1+\Omega} & 0 & 0 & -i\dfrac{q\Omega}{1+\Omega} \\ 0 & 0 & 0 & 1 \\ 0 & -i\Omega q & (1+\Omega)q^2 & 0 \end{bmatrix} \times \begin{bmatrix} y_1(x) \\ y_2(x) \\ y_3(x) \\ y_4(x) \end{bmatrix} = M\boldsymbol{y}(x) \tag{A6}$$

We seek a solution in the form $\boldsymbol{y}(x) = e^{\lambda x}\mathbf{v}$ and thus $(\mathbf{M} - \lambda\mathbf{1})\mathbf{v} = 0$, where $\lambda = -q, -q, q, q$. Following standard methods we find

$$\boldsymbol{y}(x) = c_1 e^{-qx}\begin{bmatrix} -\dfrac{i}{q} \\ i \\ -\dfrac{1}{q} \\ 1 \end{bmatrix} + c_2 e^{-qx}\begin{bmatrix} \dfrac{i}{q} + \dfrac{2i}{q\Omega} + ix \\ -\dfrac{2i}{\Omega} - iqx \\ x \\ 1 - qx \end{bmatrix}$$

$$+ c_3 e^{qx} \begin{bmatrix} -\frac{i}{q} \\ -i \\ \frac{1}{q} \\ 1 \end{bmatrix} + c_4 e^{qx} \begin{bmatrix} \frac{i}{q} + \frac{2i}{q\Omega} - ix \\ \frac{2i}{\Omega} - iqx \\ x \\ 1 + qx \end{bmatrix} \tag{A7}$$

Notice that the first and third vectors correspond to the two linear independent solutions of the above eigensystem for $-q$ and q. The other two solutions are derived from the solution of $(M - \lambda\mathbf{1})\ (M - \lambda\mathbf{1})\ \mathbf{v}_1 = 0$ (with $(M - \lambda\mathbf{1})\ \mathbf{v}_1 \neq 0$) for $-q$ and q, i.e. they are given by $\exp(\lambda x)\,(\mathbf{v}_1 + x(M - \lambda\mathbf{1})\ \mathbf{v}_1)$. Actually, in the present case we choose to construct the solution, which we are going to use below, based on both independent solutions of $(M - \lambda\mathbf{1})\ (\mathbf{M} - \lambda\mathbf{1})\ \mathbf{v}_k = 0$, i.e. $\exp(\lambda x)\,(\mathbf{v}_k + x\,(M - \lambda\mathbf{1})\ \mathbf{v}_k)$, where $k = 1, 2$. Thus

$$y(x) = c_1 e^{-qx} \begin{bmatrix} i\frac{qx\Omega + 2\Omega + 2}{\Omega} \\ -iq\frac{qx\Omega + \Omega + 2}{\Omega} \\ 1 + qx \\ -xq^2 \end{bmatrix}$$

$$+ c_2 e^{-qx} \begin{bmatrix} i\frac{qx\Omega + \Omega + 2}{q\Omega} \\ -i\frac{qx\Omega + 2}{\Omega} \\ x \\ 1 - qx \end{bmatrix}$$

$$+ c_3 e^{qx} \begin{bmatrix} i\frac{qx\Omega - 2\Omega - 2}{\Omega} \\ -iq\frac{-qx\Omega + \Omega + 2}{\Omega} \\ 1 - qx \\ -xq^2 \end{bmatrix}$$

$$+ c_4 e^{qx} \begin{bmatrix} i\frac{-qx\Omega + \Omega + 2}{q\Omega} \\ i\frac{-qx\Omega + 2}{\Omega} \\ x \\ 1 + qx \end{bmatrix} \tag{A8}$$

For the u-displacement, we consequently have

$$u(x,z) = \sum_{j=-\infty}^{\infty} \frac{ie^{izq_j}}{\Omega}\Big[c_1(j)(x\Omega q_j + 2\Omega + 2)e^{-xq_j} + c_3(j)(x\Omega q_j - 2\Omega - 2)e^{xq_j} + c_2(j)\frac{(x\Omega q_j + \Omega + 2)}{q_j}e^{-xq_j} + c_4(j)\frac{(-x\Omega q_j + \Omega + 2)}{q_j}e^{xq_j}\Big] \tag{A9}$$

First we consider the matrix displacement field for negative x (with positive q, because $u(x,z)$ must vanish for $x \to -\infty$)

$$u^-(x,z) = \frac{e^{xq_j}(x\Omega q_j - 2\Omega - 2)}{\Omega} \times [ic_3(j)e^{izq_j} - ic_1(-j)e^{-izq_j}] + \frac{e^{xq_j}(-x\Omega q_j + \Omega + 2)}{\Omega q_j} \times [ic_4(j)e^{izq_j} - ic_2(-j)e^{-izq_j}] \tag{A10}$$

Notice that we consider the single mode (single q) case. In order to be able to match the fibre displacement along the boundary we must have

$$ic_3(j) = -ic_1(-j) \text{ and } ic_4(j) = -ic_2(-j) \tag{A11}$$

and thus

$$u^-(x,z) = \frac{2ie^{xq_j}}{\Omega}\Big[(-x\Omega q_j + 2\Omega + 2)c_1(-j) - \frac{(-x\Omega q_j + \Omega + 2)}{q_j}c_2(-j)\Big]\cos(zq_j) + u_0 \tag{A12}$$

where we have added

$$-u_{0j} = \frac{2ie^{-bq_j/2}}{\Omega}\Big[\Big(\frac{b\Omega q_j}{2} + 2\Omega + 2\Big)c_1(-j) - \frac{1}{q_j}\Big(\frac{b\Omega q_j}{2} + \Omega + 2\Big)c_2(-j)\Big] \tag{A13}$$

so that the solution matches the fibre displacement (cf. Equations 14 and 19 at the boundary $x = -b/2$). Note that this displacement field is also correct for $q = 0$, i.e. $u(x,z) = 0$ for $q = 0$. Now for $u(x,z)$ on the other side of the fibre, analogous to the above, we have

$$u^+(x,z) = \frac{ie^{-xq_j}(x\Omega q_j + 2\Omega + 2)}{\Omega} \times [e^{izq_j}c_1(j) - e^{-izq_j}c_3(-j)] + \frac{ie^{-xq_j}(x\Omega q_j + \Omega + 2)}{\Omega q_j} \times [e^{izq_j}c_2(j) - e^{-izq_j}c_4(-j)] \tag{A14}$$

$$c_3(-j) = -c_1(j);\quad c_4(-j) = -c_2(j) \tag{A15}$$

$$u^+(x,z) = \frac{2ie^{-xq_j}}{\Omega}\Big[(x\Omega q_j + 2\Omega + 2)c_1(j) + \frac{(x\Omega q_j + \Omega + 2)}{q_j}c_2(j)\Big]\cos(zq_j) + u_0 \tag{A16}$$

Again we have added

$$-u_{0j} = \frac{2ie^{-bq_j/2}}{\Omega}\Big[\Big(\frac{b\Omega q_j}{2} + 2\Omega + 2\Big)c_1(j) + \frac{1}{q_j}\Big(\frac{b\Omega q_j}{2} + \Omega + 2\Big)c_2(j)\Big] \tag{A17}$$

Now we turn to the w-displacement

$$w(x,z) = \sum_{j=-\infty}^{\infty} e^{izq_j}(c_1(j)(1+xq_j)e^{-xq_j} + c_2(j)xe^{-xq_j} + c_3(j)(1-xq_j)e^{xq_j} + c_4(j)xe^{xq_j}) \quad \text{(A18)}$$

Again, we split the summation according to the solutions for negative and positive x when q_j is positive. For the case when x is negative, matching the fibre displacements at the boundary requires

$$c_3(j) = -c_1(-j); \quad c_4(j) = -c_2(-j) \quad \text{(A19)}$$

And thus

$$w^-(x,z) = -2ie^{xq_j}[(1-xq_j)c_1(-j) + xc_2(-j)]\sin(zq_j) \quad \text{(A20)}$$

Analogously

$$c_3(-j) = -c_1(-j); \quad c_4(-j) = -c_2(j) \quad \text{(A21)}$$

and

$$w^+(x,z) = 2ie^{-xq_j}[(1+xq_j)c_1(j) + xc_2(j)]\sin(zq_j) \quad \text{(A22)}$$

for positive x.

The next step is to consider the boundary conditions given by

$$4\lambda_{\xi\eta z}\left(\frac{\partial}{\partial z}u_I(z) + \frac{\partial}{\partial x}w_I(x,z)\right)\Big|_{x=\pm\frac{b}{2}} = \mu\left(\frac{\partial}{\partial z}u_{II}(x,z) + \frac{\partial}{\partial x}w_{II}(x,z)\right)\Big|_{x=\pm\frac{b}{2}} \quad \text{(A23)}$$

where the subscripts I and II denote the fibre and the surrounding medium, respectively. Using the fibre displacements

$$u_I(z) = u_0[1-\cos(qz)] \quad \text{(A24)}$$

and

$$w_I(x,z) = -qxu_0[1-\varepsilon(x)]\sin(qz) \quad \text{(A25)}$$

we obtain at $x = -b/2$

$$g_j - 2i\mu e^{-bq_j/2}\left[-2q_j\left(\frac{1}{\Omega}+\frac{bq_j}{2}+1\right)c_1(-j) + \left(\frac{2}{\Omega}+bq_j\right)c_2(-j)\right] = 0 \quad \text{(A26)}$$

and at $x = b/2$

$$g_j - 2i\mu e^{-bq_j/2}\left[-2q_j\left(\frac{1}{\Omega}+\frac{bq_j}{2}+1\right)c_1(j) - \left(\frac{2}{\Omega}+bq_j\right)c_2(j)\right] = 0 \quad \text{(A27)}$$

where g_j is above g (cf. Equation 23) with $q = q_j$. Notice that the preceding two equations together with the above conditions involving u_{0j} imply that

$$c_1(-j) = c_1(j); \quad c_2(-j) = -c_2(j) \quad \text{(A28)}$$

At this point we have all the ingredients to calculate the elastic potential energy of the matrix, which is given by

$$\pi_{\text{matrix}} = \int_0^L \int_{-\infty}^{-b/2} H_{II}^- \, dz\, dx + \int_0^L \int_{b/2}^{\infty} H_{II}^+ \, dz\, dx \quad \text{(A29)}$$

where

$$H_{II}^{\pm} = \left(\frac{\lambda}{2}+\mu\right)\left\{\left[\frac{\partial}{\partial x}\mu_{II}^{\pm}(x,z)\right]^2 + \left[\frac{\partial}{\partial z}w_{II}^{\pm}(x,z)\right]^2\right\} \quad \text{(A30)}$$

$$+ \lambda\frac{\partial}{\partial x}u_{II}^{\pm}(x,z)\frac{\partial}{\partial z}w_{II}^{\pm}(x,z) + \frac{\mu}{2}\left[\frac{\partial}{\partial x}w_{II}^{\pm}(x,z) + \frac{\partial}{\partial z}u_{II}^{\pm}(x,z)\right]^2$$

is the local elastic free energy of an isotropic medium [8]. Again we can write the result in matrix form, which leads to Equations 40–45 with

$$c_1 = ic_1(j); \quad c_2 = ic_2(j) \quad \text{(A31)}$$

References

1. H. JIANG, W. W. ADAMS and R. K. EBY, in "Material Science and Technology," Vol. 12, edited by R. W. Cahn, P. Haasen and E. J. Kramer (VCH, New York, 1993) p. 597.
2. W. W. ADAMS, R. K. EBY and D. E. MCLEMORE (eds) "The material science and engineering of rigid-rod polymers", Vol. 134 (MRS, Pittsburgh, PA, 1989).
3. W. SWEENY, *J. Polym. Sci. A Polym. Chem.* **30** (1992) 1111.
4. S. J. DETERESA, R. S. PORTER and R. J. FARRIS, *J. Mater. Sci.* **20** (1985) 1645.
5. S. S. ABRAMCHUK and V. D. PROTASOV, *Mech. Compos. Mater.* **23** (1987) 1.
6. S. G. WIERSCHKE, *Mater. Res. Symp. Proc.* **134** (1989) 313.
7. S. V. D. ZWAAG, S. J. PICKEN and C. P. V. SLUIJS, in "Integration of fundamental polymer science and technology", Vol. 3, edited by P. J. Lemstra and L. A. Kleintjens (Elsevier Applied Science, London, 1989) p. 199.
8. L. D. LANDAU and E. M. LIFSHITZ, "Theory of elasticity" (Pergamon Press, London, 1970).
9. S. P. TIMOSHENKO and J. M. GERE, "Theory of elastic stability" (McGraw-Hill, London, 1988).
10. S. J. DETERESA, S. R. ALLEN, R. J. FARRIS and R. S. PORTER, *J. Mater. Sci.* **19** (1984) 57.
11. S. V. D. ZWAAG and G. KAMPSCHOER, in "Integration of Fundamental Polymer Science and Technology", Vol. 2, edited by P. J. Lemstra and L. A. Kleintjens (Elsevier Applied Science, London, 1988) p. 545.
12. S. J. DETERESA and R. J. FARRIS, *Mater. Res Soc. Symp. Proc.* **134** (1989) 375.
13. S. KUMAR and T. E. HELMINIAK, *ibid.* **134** (1989) 363.
14. S. A. FAWAZ, A. N. PALAZOTTO and C. S. WANG, *ibid.* **134** (1989) 381.
15. F. J. MCGARRY and J. E. MOALLI, *Polymer* **32** (1991) 1816.
16. *Idem, ibid.* **32** (1991) 1811.
17. M. G. DOBB, D. J. JOHNSON and B. P. SAVILLE, *ibid.* **22** (1981) 960.
18. S. J. DETERESA, R. S. PORTER and R. J. FARRIS, *J. Mater. Sci.* **23** (1988) 1886.
19. B. W. ROSEN, *J. Am. Inst. Aero. Astron.* **2** (1964) 198.
20. "Mathematica", Vers. 2.2., *Wolfram Research* (1993).
21. S. J. DETERESA, R. S. PORTER and R. J. FARRIS, in "Composite systems from natural and synthetic polymers", edited by L. Salmén, A. deRuvo, J. C. Seferis and E. B. Stark (Elsevier Science, Amsterdam, 1986) p. 141.

Received 20 July
and accepted 21 September 1994